Dissociative Electron Attachment to DNA

X. Pan, P. Cloutier, D. Hunting, and L. Sanche*

Group of the Canadian Institutes of Health Research in the Radiation Sciences, Faculté de médecine, Université de Sherbrooke, Sherbrooke (QC) Canada J1H 5N4

(Received 8 November 2002; published 22 May 2003)

Electron-stimulated desorption of anions from thin films of linear and supercoiled DNA is investigated in the range 3–20 eV. Resonant structures are observed with maxima at 9.4 ± 0.3, 9.2 ± 0.3, and 9.2 ± 0.3 eV, respectively, in the yield dependence of H^-, O^-, and OH^- on the incident electron energy. Their formation is attributed to dissociative electron attachment.

DOI: 10.1103/PhysRevLett.90.208102 PACS numbers: 87.50.Gi, 34.50.Gb, 34.80.Ht, 87.14.Gg

Ionizing radiation induces genotoxic, mutagenic, and recombinogenic lesions in DNA, including single and double-strand breaks, base damage, and clustered damage (locally multiply damaged sites) [1]. These lesions are induced by secondary species, generated by the primary ionizing radiation. The secondary electrons of energies below 20 eV are the most abundant of these secondary species [2]. A detailed investigation of the action of secondary low-energy electrons (LEEs) is therefore crucial to comprehend the basic mechanisms by which ionizing radiation damages DNA. To reach this goal the damage induced by LEE impact on DNA [3,4] and its basic constituents (i.e., H_2O [5], bases [6], and sugar analogs [7]) has recently been investigated by various techniques.

The DNA molecule is composed of two antiparallel strands of repeated sugar-phosphate units hydrogen bonded together by the four bases, covalently linked to the sugar moiety of the backbone. The short single-stranded segments shown in Figs. 1 and 2 exhibit two sugar rings with the bases guanine and cytosine, and adenine and thymine, respectively, bonded to a phosphate unit. Under ultrahigh vacuum (UHV) conditions, DNA still contains on average 2.5 water molecules per base pair [8]; these H_2O molecules are an integral part of the DNA structure. Recently, Boudaiffa *et al.* [3,4] showed that the impact of 5–1500 eV electrons on dry DNA films produces both single (SSB) and double-strand breaks (DSB). The electron energy dependence of the yields of these breaks exhibited strong resonance features between 5 and 15 eV with a maximum between 8–10 eV. These authors concluded that most of the SSB and DSB below 15 eV are initiated by resonant electron attachment to the various components of DNA, followed by the decay of the local transient anion into dissociative channels: the dissociation of the anion (i.e., dissociative electron attachment, DEA) and/or autoionization leading to electronic excitation of a basic component in a dissociative state; e.g., for fragmentation of a covalent hydrogen bond of a basic component *R*H the damage can arise from

$$e + RH \rightarrow (RH)^- \rightarrow (RH)^* + e \rightarrow R\cdot + H\cdot + e \quad (1)$$

and/or

$$e + RH \rightarrow (RH)^- \rightarrow R\cdot + H^- \quad \text{or} \quad R^- + H\cdot . \quad (2)$$

Within a local complex potential curve crossing model, the DEA cross section to a basic component may be expressed as [9]

$$\sigma_{\text{dea}}(E) = \sigma_{\text{cap}}(E)\exp(-t/\tau_a), \quad (3)$$

where τ_a is the average lifetime towards autodetachment. The capture cross section $\sigma_{\text{cap}}(E)$ is proportional to the square of the Broglie wavelength (λ_e) of the incident electron; $t = |R_c - R_e|/v$, where R_e is the equilibrium

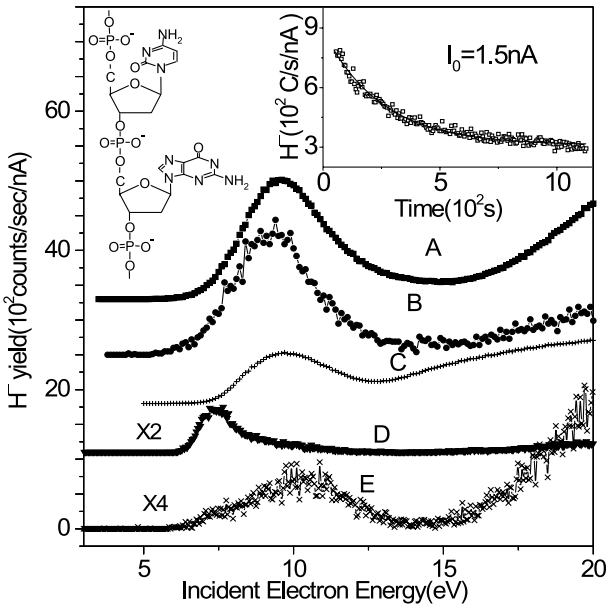

FIG. 1. Incident electron energy dependence of H^- yields (i.e., the H^- yield function) from thin films of: (*A*) double stranded linear DNA, 40 base-pairs, (*B*) supercoiled plasmid DNA, (*C*) thymine [6], (*D*) water [5], and (*E*) a ribose analog [7]. The zero-count baseline of curves *A*–*D* has been displaced for clarity. Part of a single DNA strand is shown in the upper left. The dependence of the magnitude of the H^- signal on time of exposure to the electron beam is shown by the open squares in the upper right inset. The solid line is an exponential fit to the data.

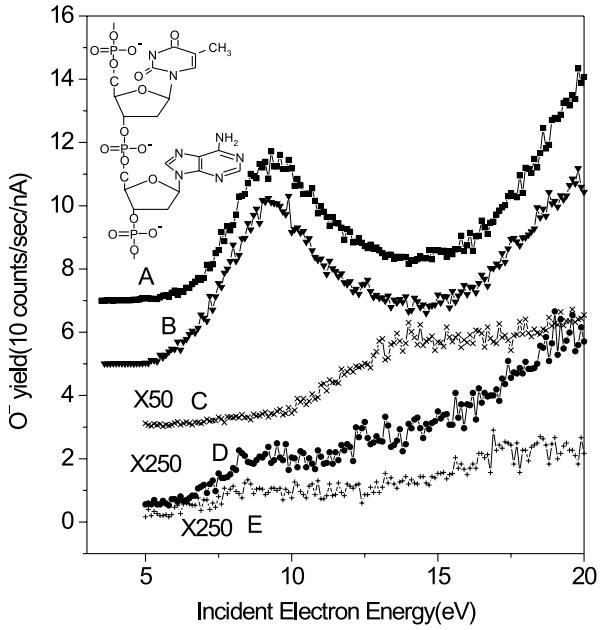

FIG. 2. O^- yield function from thin film of: (*A*) linear DNA, 40 base pairs, (*B*) supercoiled plasmid DNA, (*C*) thymine [6]. (*D*) guanine [6], and (*E*) cytosine [6]. The zero-count baseline of curves *A*–*D* has been displaced for clarity. Part of a single DNA strand is shown in the left corner at the top.

bond length of the neutral ground state of the particular component, R_c the internuclear separation along the dissociation coordinates beyond which autodetachment is no longer possible, and v the average velocity of the anion fragment in the autoionization region upon dissociation. Equation (3) defines the essential parameters of the DEA process [10]. *These parameters for an isolated basic constituent are expected to be strongly affected within DNA by the local environment of the molecule and chemical bonding,* thus changing the magnitude of the DEA cross section. In particular, λ_e will be different within DNA due to electron diffraction prior to attachment [11]. Furthermore, it has been shown that covalent bonding [12] and the presence of strong electric fields [13] can reduce the lifetime, τ_a, of electron resonances.

In this Letter, we demonstrate that DEA is involved in LEE-induced DNA damage, and exhibits a maximum intensity around 9–9.5 eV, close to the maximum in the yields of SSB and DSB induced by LEE impact on DNA [3]. The DEA process is therefore not limited to small molecules, but can also occur in an extremely large biomolecule, inducing fragmentation and producing anions and radicals. *The reported results further indicate that* H^- *produced by DEA to DNA arises principally from the bases and the sugar ring of the backbone, whereas* O^- *is produced from fragmentation of the phosphate group in the backbone.* To our knowledge, these results constitute the first *anion* mass spectroscopy measurements performed on DNA.

Two types of DNA samples were bombarded with LEE: synthetic 40-base-pair linear DNA and "natural" plasmid DNA purified from bacteria. Linear DNA was formed from complementary oligonucleotides, 40 nucleotides in length, purified by polyacrylamide gel electrophoresis. The oligonucleotides were further purified using QIAquick spin columns (Qiagen) to remove salts and other impurities. To form duplex DNA, 120 pmoles of each oligonucleotide were heated to 82 °C, in pure water and cooled to room temperature over 2.5 h in a polymerase chain reaction apparatus. Ten μl of this 40 base pair DNA solution containing 0.5 μg DNA, was deposited uniformly onto a chemically clean tantalum plate over an area of 1 cm^2. The sample was then lyophilized with a hydrocarbon-free sorption pump under a pressure of 5 mTorr. The average thickness of the film was calculated to be 2.9 ± 0.3 nm, at a known solid density of $1.7\ g \cdot cm^{-3}$, assuming that the DNA strands were lying flat on the plate; such a DNA sample is on average about 1.5 monolayers (ML) thick. Supercoiled plasmid DNA [pGEM-3Zf(−), 3197 base pairs] was purified and deposited by the same procedure as linear DNA. The thickness of the plasmid films, which consisted of 1 μg plasmid DNA, was about 3 ML. Since for both the oligonucleotides and the plasmid, the DNA bound to the QIAquick column was washed with a buffer containing sodium perchlorate and then eluted with pure water, the DNA film consisted of the sodium salt of DNA [14]. All samples were prepared in a sealed glove box under a pure dry nitrogen atmosphere and transferred to a load-lock vacuum system ($\sim 1.0 \times 10^{-8}$ Torr) for evacuation for 12 h at room temperature. Afterwards, they were transferred via a gate valve to a rotary target holder housed in an UHV chamber ($\sim 2.0 \times 10^{-10}$ Torr).

Once in the UHV chamber, the DNA sample surface was positioned perpendicular to the axis of a mass spectrometer. The sample film was irradiated by an electron gun producing a beam of 1.5 nA on a 4 mm^2 spot with an energy spread of 0.5 eV full width at half maximum. All experiments were performed at room temperature. The yields of anions desorbing at $m/e = 1$, 16, and 17 were measured as a function of incident electron energy. The 1- and 17-Da fragments could be unambiguously assigned to H^- and OH^-, but the 16-Da mass peak could arise from O^- and/or NH_2^-. However, since NH_2^- could only have originated from the bases, which have been shown to yield only O^- [6], we ascribed the 16-Da peak to O^-.

The apparatus was the same as previously used to measure H^-, O^-, and OH^- desorption from films of the DNA bases and H^- desorption from amorphous ice films. Comparison of the yields of these anions from previous experiments with those of the present experiment is valid within at least a factor of 2, for uncharged films thicker than ~10 Å [15,16]. The other H^- yield reported here for α-tetrahydrofuryl alcohol was recorded with a different instrument. In this case, the relative error could

reach a factor of 4. The incident electron energy was calibrated on the 10-eV peak in the yield function obtained from H^- desorption induced by 3–20 eV electron impact on 2-methylnaphthalene ($C_{11}H_{10}$) films [17] and by taking as 0 eV the onset of electron transmission through the film. The error on the energy scale is estimated to be ± 0.3 eV including any effects of film charging [18]. As shown in the inset of Fig. 1 for H^- desorption, all anion ESD yields decrease exponentially as a function of time of exposure. This exponential behavior reflects the depletion of the original molecules, thus indicating that the measured desorption yields are directly proportional to the number of intact targets (i.e., we are observing a primary process). Any significant desorption from secondary processes would therefore modify this behavior.

Electron bombardment of 40-base-pair DNA and plasmid DNA films produces H^-, O^-, and OH^- as the major anion desorption signals. The incident electron energy dependence of the H^-, O^-, and OH^- yields (i.e., the yield functions) from 40-base-pair DNA is shown in *A* of Figs. 1–3, respectively. The energy thresholds for producing these anions are 4.5, 4.7, and 4.9 eV, respectively. The yield functions for H^-, O^-, and OH^- exhibit a single broad peak near 9 eV with a continuous rise at higher energy. The results obtained from LEE-bombarded films of "natural" DNA, shown in *B* of Figs. 1–3, exhibit essentially the same characteristics as those appearing in *A*. Both results are therefore interpreted similarly. The prominent 9-eV feature in *A* and *B* of Figs. 1–3 is a typical signature of the DEA process. In fact, below the threshold for dipolar dissociation (identified here as the continuous rise in signal that onsets near 15 eV), DEA is the only mechanism that can produce anion fragments [15,19]. The maxima at, respectively, 9.4, 9.2, and 9.2 eV in the H^-, O^-, and OH^- yield function from DNA correlate well with the maximum spreading from 8 to 10 eV in the SSB yields and the one occurring at 10 eV in the DSB yields induced by LEE impact on films of supercoiled DNA [3]. At energies as high as 10 eV, DEA occurs via the dissociation of a transient anion resulting from the capture of an electron by the positive electron affinity of an electronically excited state. We therefore expect the additional electron to attach to an electronically excited state of a basic constituent of DNA, in agreement with the conclusion of Boudaiffa *et al.* [3]. According to Eq. (3), the transient anions formed from the constituents retain a sufficiently long lifetime within DNA to allow substantial anion desorption.

Curves *C*, *D*, and *E* shown in Fig. 1 exhibit the H^- yield functions from films of thymine, amorphous ice, and α-tetrahydrofuryl alcohol having thicknesses larger than 12 Å [5–7]. The results obtained for the three other bases are similar to that of thymine [6]. Those obtained from tetrahydrofuran (i.e., the sugar ring in DNA) and its DNA backbone sugarlike analogs [7] are essentially the same as that shown in Fig. 1, curve *E*. This previous result

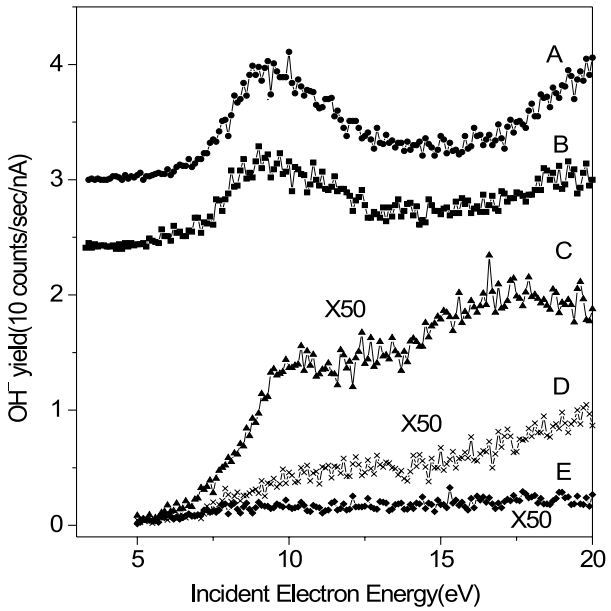

FIG. 3. OH^- yield function of the same films as in Fig. 2. The zero-count baseline of curves *A* and *B* has been displaced for clarity.

indicates that DEA to the ring is the main H^- desorption pathway. The H^- peak energy from amorphous water in *D* is definitively too low to be associated with DEA to the structural H_2O of DNA, unless the strong hydrogen bonding in DNA shifts considerably the H_2O^- resonance energy. In contrast, comparison of curve *C* with curves *A* and *B* in Fig. 1, indicates that the bases are important sources of H^- desorption with an intensity about 3 times that arising from the sugar ring (Fig. 1, curve *E*). Thus, comparison of the line shapes of the yield functions and their intensities in Fig. 1 suggests that LEE-induced H^- desorption from DNA below 15 eV occurs mainly via DEA to the bases with an important contribution from the ribose ring.

The difference in magnitude of the H^- signal intensity between curves *A*, *B* and *C*, *E* in Fig. 1 may be ascribed to changes in the density of each component in the films and modification of the intrinsic properties of the local transient anion in DNA described by Eq. (3) and also the extrinsic properties [20]. Both properties are affected by the different nature of the films, the presence of electric fields, and covalent bonding of the constituents in DNA. The latter two should have a strong influence on the intrinsic properties, particularly the anion's lifetime, on which the magnitude of DEA depends exponentially [9,20]. Furthermore, since the capture probability depends on the electron wavelength and the lifetime, it may be also considerably modified by diffraction, bonding, and local electric fields within DNA. The extrinsic properties depend on the image force and scattering of the desorbing anion [20]. They are therefore more related to the physical properties of the film. Interestingly, *the*

different topologies of the DNA (i.e., linear in A and supercoiled in B), and therefore the different physical nature of the DNA film, does not seem to affect the desorption intensity of any of the major anions detected. This result further indicates that the measured yields result from a local interaction (e.g., DEA to a basic constituent) not related to the long range geometrical properties of DNA.

In their electron impact experiments on films of DNA backbone sugar analogs, Antic *et al.* [7] did not observe any desorption of O^-, and OH^-. *Similarly, LEE impact on ice films does not desorb* O^- and OH^- *anions* [21]. Curves *A* and *B* in Figs. 2 and 3 cannot, therefore, be easily interpreted by invoking a DEA reaction on these DNA components. On the other hand, the O^- signal from ~15 Å films of those DNA bases, which contain oxygen (i.e., thymine, cytosine, and guanine), show that O^- desorption via DEA around 20 eV is at least 2 orders of magnitude smaller than the O^- signal from DNA near the same energy. Furthermore, the line shapes of these O^- yield functions bear little resemblance to those of curves *A* and *B* in Fig. 2. Hence, it appears that the relatively large O^- signal from DNA does not arise from DEA to the bases since covalent bonding [12] should decrease the transient anion lifetime and according to Eq. (3) decrease exponentially the DEA cross section. The only other and most likely possibility is DEA to the phosphate group (PO_4). In this case, electron capture is expected to occur within a π^* orbital on the O═P bond [22], since in the vicinity of the O^- counterion the electric field may be too strong for transient anions to dissociate before autoionization.

The OH^- signal from thymine is at least an order of magnitude smaller than that from DNA as seen from comparison of curves *A* and *B* to *C* in Fig. 3. The contribution from the other bases (*D* and *E*) is even smaller. Furthermore, the OH^- yield functions of the bases are different than those seen from DNA, indicating here again, that the OH^- signal from DNA probably does not arise from the bases. However, a portion of the OH^- signal could arise from reactive scattering of O^- produced at the phosphate group (i.e., $O^- + C_5H_7O \rightarrow C_5H_7O_2^- \rightarrow C_5H_6O + OH^-$) [23]. In fact, Mozejko *et al.* [24] have recently shown that when oxygen is seeded into a film of tetrahydrofuran or its sugarlike analogs, OH^- is desorbed with an efficiency of a few percent of the O^- yield at 10 eV. Their interpretation in terms of reactive scattering was based on the previous observation of such reactions in alkane-O_2 mixture films [13,25]. Within DNA, O^- leaving PO_4 could therefore react with the nearby sugar moiety and contribute to OH^- desorption from DNA. In this case, the O^- and OH^- yield functions should exhibit the same behavior, with the OH^- yield being considerably smaller than that of O^-, as observed experimentally (curves *A* and *B* in Figs. 2 and 3).

Finally, we note that due to the large abundance of 0–15 eV electrons produced by high-energy radiation, the present results point to an important role for DEA in the nascent stages of DNA radiolysis within cells. Since DEA reactions are sensitive to their environment [20], they offer a mechanism to manipulate the effects of radiation at the molecular level.

We thank S. Girouard and S. Cecchini for purifying and preparing the DNA samples, Dr. A. Bass and Dr. Q. B. Lu for valuable discussions, and F. Martin for technical help. This research was supported by the Canadian Institutes of Health Research.

*Canada Research Chair in the Radiation Sciences.

[1] C. von Sonntag, *The Chemical Basis for Radiation Biology* (Taylor and Francis, London, 1987).
[2] J. A. LaVerne and S. M. Pimblott, Radiat. Res., **141**, 208 (1995); V. Cobut *et al.*, Radiat. Phys. Chem. **51**, 229 (1998).
[3] B. Boudaiffa *et al.*, Science **287**, 1658 (2000).
[4] B. Boudaiffa *et al.*, Int. J. Radiat. Biol. **76**, 1209 (2000).
[5] P. Rowntree, L. Parenteau, and L. Sanche, J. Chem. Phys. **94**, 8570 (1991); W. C. Simpson *et al.*, J. Chem. Phys. **107**, 8668 (1997).
[6] H. Abdoul-Carime, P. Cloutier, and L. Sanche, Radiat. Res. **155**, 625 (2001).
[7] D. Antic *et al.*, J. Phys. Chem. B **103**, 6611 (1999).
[8] S. G. Swarts *et al.*, Radiat. Res. **129**, 333 (1992).
[9] T. F. O'Malley, Phys. Rev. **150**, 14 (1966).
[10] L. Sanche, Surf. Sci. **451**, 82 (2000).
[11] G. Bader and L. Sanche, Phys. Rev. B **30**, 78 (1984).
[12] M. Gruyters and K. Jacobi, Surf. Sci. **336**, 314 (1995).
[13] L. Sanche and L. Parenteau, J. Chem. Phys. **93**, 7476 (1990).
[14] B. Vogelstein and D. Gillespie, Proc. Natl. Acad. Sci. U.S.A. **76**, 615 (1979).
[15] L. Sanche, Scanning Microsc. **9**, 619 (1995).
[16] M.-A. Hervé du Penhoat *et al.*, J. Chem. Phys. **114**, 5755 (2001).
[17] P. Rowntree, L. Parenteau, and L. Sanche, J. Phys. Chem. **95**, 523 (1991); X. Pan and L. Sanche (unpublished).
[18] K. Nagesha *et al.*, Rev. Sci. Instrum. **68**, 3883 (1997).
[19] L. Sanche, Phys. Rev. Lett. **53**, 1638 (1984).
[20] M. A. Huels, L. Parenteau, and L. Sanche, J. Chem. Phys. **100**, 3940 (1994).
[21] P. Rowntree, L. Parenteau, and L. Sanche, J. Chem. Phys. **94**, 8570 (1991); W. C. Simpson and L. Sanche, J. Chem. Phys. **108**, 5027 (1998).
[22] W. L. Jorgensen and L. Salem, *The Organic Chemist's Book of Orbitals* (Academic Press, New York, 1973).
[23] A. Bass *et al.*, J. Chem. Phys. **109**, 8635 (1998).
[24] P. Mozejko *et al.* (to be published).
[25] L. Sanche and L. Parenteau, Phys. Rev. Lett. **59**, 136 (1987).